

the product $\text{Cp}_2\text{Fe}_2(\text{PMe}_2\text{Ph})(\text{CO})(\mu\text{-CO})(\mu\text{-CSMe})^+$ at -1.14 V. On the second cycle the -0.78 -V wave becomes smaller while the -1.14 V wave grows. The voltammogram is essentially unchanged for additional cycles. Thus, the substitution reaction (eq 3) is complete after one cycle. The CV of a stirred solution of **1** and PMe_2Ph shows no anodic waves corresponding to either cathodic peak, indicating that reduced species are not adsorbed to the electrode. The CV of **1** in the presence of **4** equiv of PMe_2Ph is essentially the same as with only 1 equiv. Likewise, the CV of **1** in the presence of 8 equiv of PEt_3 is essentially the same as for PMe_2Ph . This insensitivity of the cyclic voltammograms to the nature and concentration of the phosphine requires the rate of reaction 3 to be independent of the phosphine. This would be true in the mechanism, eq 4-7, if $k_2[\text{L}] \gg k_{-1}[\text{CO}]$; then, the rate law (8) would reduce to $d[\mathbf{9}]/dt = k_1[\mathbf{2}]$, and the rate-determining step would be the dissociation of CO from **2**. This is apparently the case for the ligands (PEt_3 , PMePh_2 , PMe_2Ph , and $t\text{-BuNC}$) that have essentially the same current efficiencies (~ 40 mol/faraday in Table I).

The lower current efficiency for the PPh_3 reaction suggests that $k_2[\text{L}]$ is not larger than $k_{-1}[\text{CO}]$ and that CO competes effectively

with PPh_3 for the coordinatively unsaturated intermediate **3**. In this case, decomposition of **2** would be expected; indeed products of its decomposition are observed.

While detailed kinetic studies of reaction 3 have not been performed, the observed CV's for **1** in the presence of phosphines are similar to computer-simulated CV's²⁴ based on radical chain mechanisms of the type in eq 4-7. Although there have been several recent examples^{23,25} of metal carbonyl substitution reactions which are catalyzed by chemically or electrochemically generated radicals, the present study is the first involving a dinuclear bridging carbene complex and the first in which the carbene radical is sufficiently stable to be spectroscopically characterized.

Acknowledgment. We thank the National Science Foundation (Grants CHE-8100419 and CHE-8401844) for support of this research and Dr. D. C. Johnson for helpful discussions.

(24) Feldberg, S. W.; Jestic, L. *J. Phys. Chem.* **1972**, *76*, 2439.

(25) (a) Geiger, W. E.; Connelly, N. G. *Adv. Organomet. Chem.* **1984**, *23*, 1. (b) Geiger, W. E.; Connelly, N. G. *Adv. Organomet. Chem.* **1985**, *24*, 87. (c) Geiger, W. E. *Prog. Inorg. Chem.* **1985**, *33*, 275.

Preferred Geometry of Cation-Amide Bonding. Crystal Structures of $[\text{Mg}(\text{NMA})_2(\text{H}_2\text{O})_4](\text{NO}_3)_2$ and $\text{Ca}(\text{NO}_3)_2 \cdot 4\text{NMA}$ (NMA = *N*-Methylacetamide)

Krzysztof Lewinski¹ and Lukasz Lebioda*²

Contribution from the Chemistry Department, University of South Carolina, Columbia, South Carolina 29208, and the Chemistry Department, Jagellonian University, ul Karasia 3, Krakow 30-060, Poland. Received November 7, 1985

Abstract: Complexes of *N*-methylacetamide with calcium and magnesium nitrate were studied by X-ray crystallography and IR spectroscopy. Changes in the bond lengths of the amide moiety due to cation-ligand interaction are less than 0.01 Å. A survey of the structures of cation complexes with monodentate, nonbridging amide ligands coordinated through the amide oxygen atom was carried out. It showed that for small cations with M-O distance less than 2.15 Å, there is a preferred geometry of cation-amide binding. It is in the amide plane, trans to the amide N atom and with a M-C=O angle of $135 \pm 15^\circ$. For larger cations the geometry of cation-ligand binding is closer to the direction of the dipole moment of the amide group and in general is less restricted.

Recent interest in the studies of complexes of amides with alkaline-earth cations has been stimulated by the physiological importance of Mg^{2+} and Ca^{2+} and the use of amides like NMA³ as models for polypeptide-cation binding. Peptide carbonyls are frequent ligands in protein- Ca^{2+} complexes⁴ and in some ionophores⁵ and also were implicated in the mechanism of membrane ion pumps.⁶ Complexes of alkali-metal and alkaline-earth cations with amides have been extensively studied by vibrational and NMR spectroscopy, quantum mechanics calculations,⁷ and X-ray crystallography⁸ with the objective being the determination of the

mode of binding, ligand polarization, and the effect of lone electron pairs on the geometry of bonding. It was found that invariably the carbonyl oxygen is the metal coordination site and that polarization of the amide leads to a shift of electron density from the amide N atom to the O atom and the consequently decrease of the double bond character of the C=O bond and an increase of the double bond character of the C-N bond. The degree of polarization varied with ionic radius for both alkali-metal and alkaline-earth cations series, but the relation between those series depends on the method used. Rao and co-workers^{8,9} studied by X-ray crystallography structures of several complexes of alkali-metal and alkaline-earth cations with NMA and DMF and tried to correlate the observed changes between the bond lengths. All their data, however, were of relatively low precision, and in addition anions with weak H-bond accepting properties were used. To verify their hypothesis we have obtained new complexes of NMA with magnesium and calcium nitrate and carried out their structure

(1) Jagellonian University.

(2) University of South Carolina.

(3) Abbreviations used: NMA, *N*-methylacetamide; DMF, *N,N*-dimethylformamide.

(4) Szebenyi, D. M. E.; Obendorf, S. K.; Moffat, K. *Nature (London)* **1981**, *294*, 327-332.

(5) VanRoey, P.; Smith, G. D.; Duax, W. L.; Umen, M. J.; Maryanoff, B. E. *J. Am. Chem. Soc.* **1982**, *104*, 5661-5666.

(6) Urry, D. W.; Trapani, T. L.; Walker, J. T.; Prasad, K. U. *J. Biol. Chem.* **1982**, *257*, 6659-6661.

(7) Over 20 articles on this topic are in: *Metal-Ligand Interactions in Organic Chemistry and Biochemistry*; Pullman, B., Goldblum, N., Eds.: D. Reidel: Dordrecht, 1977.

(8) Chakrabarti, P.; Venkatesan, K.; Rao, C. N. R. *Proc. R. Soc. London, Ser. A* **1981**, *A375*, 127-153.

(9) Pulla Rao, Ch.; Muralikrishna Rao, A.; Rao, C. N. R. *Inorg. Chem.* **1984**, *23*, 1080-1085.

Table I. Fractional Atomic Coordinates with Esd's in Parentheses and Equivalent Isotropic Temperature Factors for $[\text{Mg}(\text{NMA})_2(\text{H}_2\text{O})_4](\text{NO}_3)_2$

	<i>X/a</i>	<i>Y/b</i>	<i>Z/c</i>	<i>B, Å</i>
Mg	0.0000 (0)	0.0000 (0)	0.0000 (0)	1.28
O(1)	0.0271 (1)	0.0848 (1)	0.0886 (0)	1.63
C(1a)	0.0181 (2)	0.0766 (1)	0.1528 (1)	1.39
C(2)	0.0351 (3)	-0.0252 (1)	0.1897 (1)	2.17
N(1a)	-0.0060 (2)	0.1601 (1)	0.1916 (1)	1.72
C(3)	-0.0227 (3)	0.2623 (1)	0.1623 (1)	2.42
C(1b)	0.0115 (33)	0.1349 (18)	0.1517 (12)	1.52
N(1b)	0.0142 (25)	0.0764 (13)	0.2004 (10)	2.04
N(2)	0.0066 (2)	0.1472 (1)	0.3824 (1)	1.38
O(21)	0.0326 (2)	0.0546 (1)	0.3670 (1)	1.96
O(22)	-0.0269 (2)	0.2129 (1)	0.3377 (1)	2.16
O(23)	0.0145 (1)	0.1751 (1)	0.4456 (0)	1.53
O(3)	0.2656 (2)	0.0631 (1)	-0.0356 (1)	1.55
O(4)	-0.1638 (2)	0.1255 (1)	-0.0386 (1)	1.51
H(21)	0.031 (2)	-0.020 (1)	0.236 (1)	2.5
H(22)	0.152 (3)	-0.055 (1)	0.177 (1)	3.4
H(23)	-0.071 (3)	-0.066 (2)	0.175 (1)	3.6
H(1a)	-0.010 (2)	0.155 (1)	0.236 (1)	2.7
H(31)	0.093 (3)	0.289 (2)	0.147 (1)	4.8
H(32)	-0.122 (3)	0.265 (2)	0.131 (1)	5.5
H(33)	-0.064 (4)	0.306 (2)	0.194 (1)	6.7
HO(31)	0.331 (3)	0.092 (1)	-0.011 (1)	2.7
HO(32)	0.335 (3)	0.028 (2)	-0.061 (1)	3.6
HO(41)	-0.245 (3)	0.143 (1)	-0.011 (1)	2.7
HO(42)	-0.104 (3)	0.177 (1)	-0.049 (1)	2.1
H(1b)	0.003 (0)	0.107 (0)	0.248 (0)	3.2

determination at low temperature.

Effect of lone electron pairs of the ligand could be investigated by an analysis of a large sample of observed geometries of cation-ligand binding.¹⁰ A thorough survey of Ca^{2+} complexes with carbonyl ligands did not show significant preference for binding along lone electron pairs although some tendency for calcium ions to lie near carbonyl planes was noted.¹¹ On the other hand, an analysis of the geometry of hydrogen bonding demonstrated a pronounced effect on lone electron pairs of sp^2 - and sp^3 -hybridized O atoms.¹² We study, therefore, the geometry of cation-amide binding as a function of cation radius.

Experimental Section

Crystals of $[\text{Mg}(\text{NMA})_2(\text{H}_2\text{O})_4](\text{NO}_3)_2$ were obtained by slow cooling of a saturated butanol-water solution of magnesium nitrate and NMA in a molar ratio of 1:4. The crystals were hygroscopic and when not protected dissolved in air moisture. They are orthorhombic: space group *Pbca*, $a = 6.603$ (1) Å, $b = 12.934$ (2) Å, $c = 19.397$ (3) Å, $V = 1657$ Å³, $Z = 4$, $D_c = 1.470$ g cm⁻³. A single crystal (0.3 × 0.2 × 0.1 mm) was used, and a total of 4409 reflections (4119 with positive intensity) were measured in a range $2^\circ < \theta < 30^\circ$ on an Enraf-Nonius CAD-4 diffractometer with graphite-monochromated Mo K α radiation at temperature 143 K. Symmetry averaging provided 2331 independent reflections and $R_{\text{sym}} = 0.028$. Intensities were corrected for Lorentz and polarization factors but not for absorption, $\mu(\text{Mo K}\alpha) = 1.64$ cm⁻¹. Two-hundred and forty reflections with $F < 3\sigma(F)$ were omitted, leaving 2091 observations. The structure was solved by the superposition method in Patterson space. Anisotropic thermal parameters for non-hydrogen atoms and isotropic for H atoms, which were located during early stages of Fourier refinement, were refined by least squares. The refinement converged at $R = 0.053$, $R_w = 0.043$. However, on the difference Fourier map there were two peaks of about 1 e/Å³ which we interpreted as arising from a low-occupancy partial disorder of the NMA ligand. The molecules of NMA occupy one coordination site in two positions denoted A (major) and B (minor) with the pairs of atoms O(1A)-O(1B), C(2A)-C(2B), C(3A)-C(3B) superimposed or very close. Two other pairs of atoms, C(1A)-C(1B) and N(1A)-N(1B), do not superimpose and that resulted in the additional peaks. This type of disorder was previously found in the room-temperature structure of crystalline NMA¹³ and almost all of its complexes.⁸ Least-squares refinement of the model

Table II. Fractional Atomic Coordinates with Esd's in Parentheses and Equivalent Isotropic Temperature Factors for $\text{Ca}(\text{NO}_3)_2 \cdot 4\text{NMA}$

	<i>X/a</i>	<i>Y/b</i>	<i>Z/c</i>	<i>B, Å</i>
Ca	0.0000 (0)	0.0000 (0)	0.0000 (0)	3.62
O(1a)	0.1082 (11)	0.1779 (14)	-0.0542 (13)	6.95
C(1a)	0.2064 (8)	0.2470 (12)	-0.0739 (10)	4.91
C(2a)	0.3268 (11)	0.2401 (19)	0.0016 (11)	11.19
N(1a)	0.2109 (8)	0.3257 (7)	-0.1651 (6)	7.37
C(3a)	0.1056 (14)	0.3325 (16)	-0.2498 (13)	8.24
O(1b)	0.2081 (14)	-0.0998 (8)	0.0339 (11)	5.16
C(1b)	0.2706 (14)	-0.1665 (9)	0.1069 (13)	7.04
C(2b)	0.3597 (18)	-0.1065 (14)	0.1968 (15)	10.48
N(1b)	0.2878 (8)	-0.2909 (10)	0.0839 (7)	9.53
C(3b)	0.2046 (12)	-0.3598 (11)	0.0017 (14)	9.38
N(2)	0.0000 (0)	0.0000 (0)	0.2583 (3)	5.56
O(21)	0.0000 (0)	0.0000 (0)	0.3661 (2)	7.57
O(22)	0.0463 (2)	0.0940 (2)	0.2015 (2)	6.37

with the two additional atoms having isotropic temperature parameters produced the occupancy ratio of the two position 0.922 (5):0.078 (5) and $R = 0.045$, $R_w = 0.036$; the highest peak in the final difference Fourier map was 0.30 e/Å³. The atomic coordinates for this model of the structure are given in Table I.

Crystals of $\text{Ca}(\text{NO}_3)_2 \cdot 4\text{NMA}$ were obtained by slow cooling of a saturated butanol-water solution of calcium nitrate and NMA in a molar ratio of 1:6. They are tetragonal: space group *P4₂1c*, $a = 10.282$ (2) Å, $c = 11.372$ (4) Å, $V = 1202$ Å³, $Z = 2$, $D_c = 1.261$ g cm⁻³. A crystal of dimensions 0.3 × 0.2 × 0.2 mm was used for data collection carried out at temperature 193 K. The same equipment and procedures were used as for the Mg^{2+} complex. Reflections measured (2148) 1433 with positive net intensity, yielded 1195 symmetry independent observations and $R_{\text{sym}} = 0.028$. None of the (*hhl*) reflections with $l = 2n + 1$ and (*h00*) reflections with $h = 2n + 1$ were above $3\sigma(F)$. Reflections (1001) with $F > 3\sigma(F)$ were used in structure solving and refinement. The structure was solved by the Patterson and Fourier method. It was immediately apparent that the molecules of NMA were also disordered and that there is no significant preference for one of the two positions. In the process of refinement it was found that in this structure the superposition of O(1) atoms and C(2)-C(3) pairs is not exact and the atom positions can be resolved. The free atom refinement of the disordered model has suffered from high correlations between the parameters; the geometry of the NMA molecules deviated from that found in the Mg^{2+} complex much more than could be due to different environment in the crystals. As discussed below, the distortions of the NMA molecules in the crystal field are very small. Thus it was apparent that those deviations are artifacts, most probably due to the parameter correlations. Therefore, to obtain a better estimation of intermolecular geometry, we utilized the knowledge of the geometry of the NMA ligands, determined in the more favorable case, using the technique of restrained refinement.¹⁴ The target values of bond lengths and angles, for the NMA molecules only, were based on values found for the Mg^{2+} complex. Anisotropic thermal parameters were used for non-H atoms. Hydrogen atoms in calculated positions were introduced, but their parameters were not refined. The refinement converged at $R = 0.052$, $R_w = 0.038$, and the largest deviation from the target value of restraint was 0.002 Å, which effectively corresponds to the rigid body refinement of the NMA molecules. The occupancy ratio of the two disordered positions converged at 0.507 (12):0.493 (12). The highest peak on the final Fourier map was 0.40 e/Å³ in the vicinity of the Ca position. The coordinates of the atoms are given in Table II.

A phase transition was observed at a lower temperature, but it was not investigated further since unfortunately it also led to single crystal-polycrystal transformation. It is quite possible that this phase transition involves ordering of the NMA molecules as is observed in NMA crystals at 283 K.¹³ We crystallized $\text{Ca}(\text{NO}_3)_2 \cdot 4\text{NMA}$ again at 253 K and mounted and transferred crystals on the diffractometer at this temperature, but the crystals were in the same disordered form.

Solid-state IR data were recorded at room temperature with a Digilab FTS-14 spectrophotometer.

Results and Discussion

Crystal Structures. The structure of the Mg^{2+} complex, despite the minor disorder observed, is probably the most precise determination of the structure of a NMA complex. The quality of the

(10) Ferraris, G.; Franchini-Angela, M. *Acta Crystallogr., Sect. B* **1972**, *B28*, 3572-3583. Lebioda, L. *Ibid.* **1980**, *B36*, 271-275.

(11) Einspahr, H.; Bugg, C. E. *Met. Ions Biol. Syst.* **1984**, *17*, 51-97.

(12) Murray-Rust, P.; Glusker, J. P. *J. Am. Chem. Soc.* **1984**, *106*, 1018-1025.

(13) Katz, J. L.; Post, B. *Acta Crystallogr.* **1960**, *13*, 624-628.

(14) The restrained refinement and most of the other calculations were done with a system of programs SHELX-76 written by G. M. Sheldrick, University of Cambridge, England, 1976.

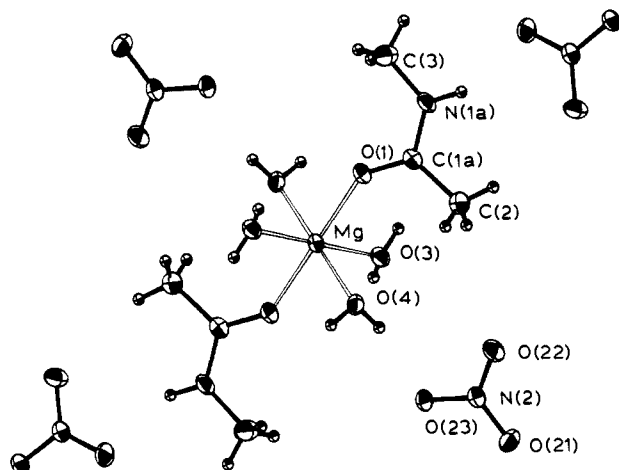


Figure 1. $[\text{Mg}(\text{NMA})_2(\text{H}_2\text{O})_4](\text{NO}_3)_2$ complex with NMA ligand in position A.

Table III. Interatomic Distances (Å) and Bond Angles (deg) with Esd's in Parentheses for $[\text{Mg}(\text{NMA})_2(\text{H}_2\text{O})_4](\text{NO}_3)_2$

Mg–O(1)	2.047 (1)	N(2)–O(21)	1.246 (2)
Mg–O(3)	2.054 (1)	N(2)–O(22)	1.234 (2)
Mg–O(4)	2.089 (1)	N(2)–O(23)	1.279 (2)
O(1)–C(1a)	1.251 (2)	O(1)–C(1b)	1.39 (2)
C(1a)–C(2)	1.503 (2)	C(1b)–C(3)	1.68 (2)
C(1a)–N(1a)	1.326 (2)	C(1b)–N(1b)	1.21 (3)
N(1a)–C(3)	1.443 (2)	N(1b)–C(2)	1.34 (2)
O(1)–Mg–O(3)	89.7 (0)	O(21)–N(2)–O(22)	121.2 (2)
O(1)–Mg–O(4)	86.0 (0)	O(21)–N(2)–O(23)	119.7 (1)
O(3)–Mg–O(4)	90.7 (1)	O(22)–N(2)–O(23)	119.1 (1)
Mg–O(1)–C(1a)	141.8 (1)		
Mg–O(1)–C(1b)	169.6 (9)		
O(1)–C(1a)–C(2)	123.0 (1)	O(1)–C(1b)–C(3)	125 (2)
O(1)–C(1a)–N(1a)	120.1 (1)	O(1)–C(1b)–N(1b)	113 (2)
C(2)–C(1a)–N(1a)	116.9 (1)	C(3)–C(1b)–N(1b)	121 (2)
C(1a)–N(1a)–C(3)	122.1 (1)	C(2)–N(1b)–C(1b)	120 (2)

structure of the Ca^{2+} complex is of inferior precision, as could be judged from the temperature parameters, despite all the precautions taken. We believe that the model refined is an approximate one and that the actual fine position of a NMA ligand in let's say the A orientation depends on whether its neighbors are in the A or B position. Therefore, in this structure we discuss only gross features.

The coordination of Mg^{2+} shown in Figure 1 is slightly distorted octahedral with Mg–O distances of 2.046–2.084 Å which fall in the normal range.¹⁵ Important bond lengths and angles are in Table III.

The complex is charge separated, and nitrate anions are hydrogen bonded to NMA and H_2O molecules. To estimate the effect of polarization on the geometry of NMA, we compare its structure (at 143 K) with the structure of acetamide determined at 27 K¹⁶ in which the amide is polarized only by hydrogen bonding. The data are given (in Å) first for the Mg complex and then for acetamide: C=O, 1.251 (2), 1.247 (1); C–N, 1.326 (2), 1.335 (1); C–C, 1.503 (2), 1.509 (1). The observed differences are quite subtle. Changes of C=O and C–N bond lengths qualitatively support the generally accepted idea of a decrease in the double bond character of C=O and an increase of C–N but indicate that previously reported measurements⁸ were interpreted well beyond their precision. The observed difference in the C–C bond length is in fact opposite to the trend proposed earlier. Indeed as a result of peptide bond polarization, the positive charge on the carbonyl carbon is larger, and that should lead to an increase of electron density in the C–C bond and a shorter distance as observed here. Rather than discuss quantitatively the

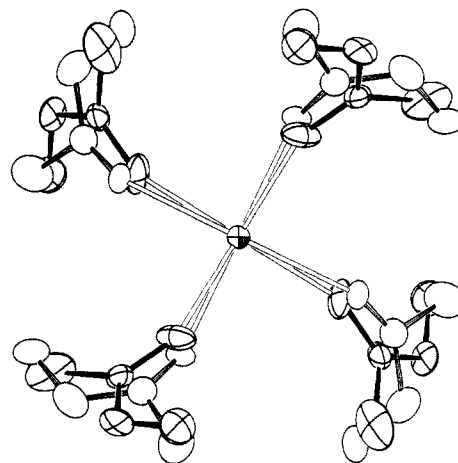
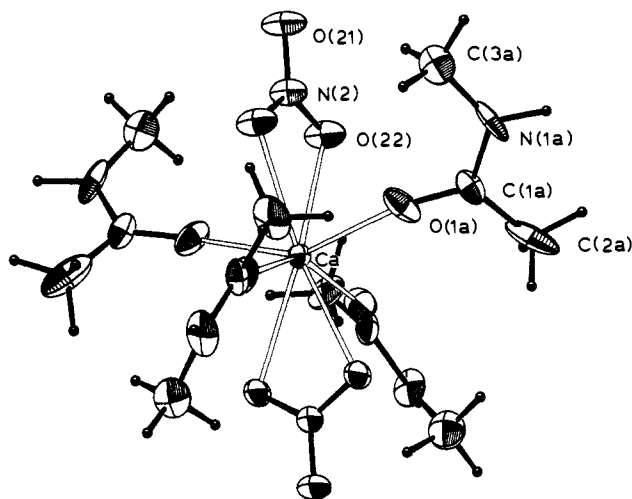


Figure 2. $\text{Ca}(\text{NO}_3)_2 \cdot 4\text{NMA}$ complex: (a, top) with NMA ligands in position A, position B omitted; (b, bottom) with disordered NMA ligands, heavier drawn are ligands in position A, nitrate anions are omitted.

changes, we want to underline the fact that contrary to the previously reported data,⁸ the changes of the bond lengths in the cation field are small, all less than 0.01 Å.

The structure of $\text{Ca}(\text{NO}_3)_2 \cdot 4\text{NMA}$ is built of charge-balanced complexes shown in Figure 2. Eight oxygen atoms in the first coordination zone of the Ca^{2+} cation form a distorted dodecahedron of symmetry $\bar{4}$. It is interesting to note that in the series of analogous compounds of general formula $\text{Ca}(\text{NO}_3)_2 \cdot 4\text{L}$ when $4\text{L} = 4\text{H}_2\text{O}$, the coordination number $\text{CN} = 9$,¹⁷ when $4\text{L} = 3\text{H}_2\text{O}$ and 1 urea, $\text{CN} = 8$,¹⁸ when $4\text{L} = 4\text{CH}_3\text{OH}$, $\text{CN} = 8$,¹⁹ when $4\text{L} = 4\text{NMA}$, $\text{CN} = 8$; when $4\text{L} = 2\text{NMA}$ and $2\text{H}_2\text{O}$, $\text{CN} = 8$,²⁰ and when $4\text{L} = 4$ urea, $\text{CN} = 6$.²¹ In all these structures the complexes are charge balanced and the variation of the coordination number is a result of a different mode of nitrate anion binding, chelating and bridging for $\text{CN} = 9$, chelating for $\text{CN} = 8$, and monodentate for $\text{CN} = 6$.

The most striking observation for complexes of Ca^{2+} and Mg^{2+} is that in Ca^{2+} complexes (three structures, six symmetry-independent ligands), the molecules of NMA are invariably heavily disordered, while in Mg^{2+} complexes (two structures, four ligands) there is no disorder or at least a 12:1 preference was found for the mode of binding where the cation is trans to the N atom.

Survey of the Geometry of Cation–Amide Bonding. Among factors which influence the orientation of an amide ligand with respect to the cation are the effect of lone electron pairs on the

(17) Leclaire, A.; Monier, J.-C. *Acta Crystallogr., Sect. B* 1977, B33, 1861–1866.

(18) Lebioda, L. *Pol. J. Chem.* 1972, 43, 373–379.

(19) Leclaire, A. *Acta Crystallogr., Sect. B* 1974, B30, 2259–2260.

(20) Lebioda, L. unpublished data.

(21) Lebioda, L. *Acta Crystallogr., Sect. B* 1977, B33, 1583–1585.

(15) Poonia, N. S.; Bajaj, A. V. *Chem. Rev.* 1979, 79, 389–445.

(16) Jeffrey, G. A.; Ruble, J. R.; McMullan, R. K.; DeFrees, D. J.; Binkley, J. S.; Pople, J. A. *Acta Crystallogr., Sect. B* 1980, B36, 2292–2299.

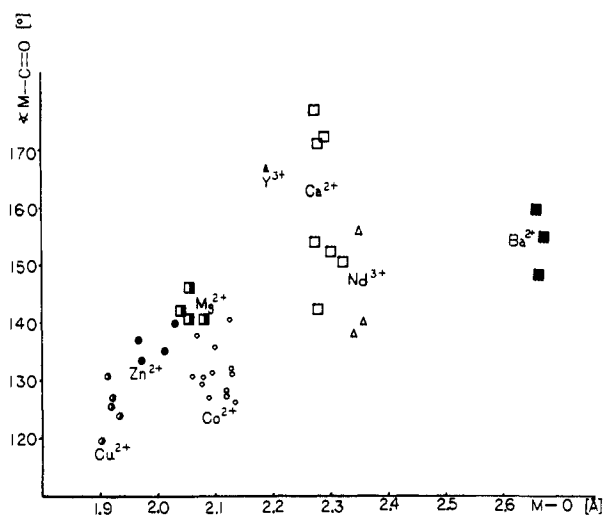


Figure 3. Entry angle $M-O=C$ in degrees as a function of the $M-O$ distance. Only monodentate, nonbridging ligands are represented here.

O atom and the electrostatic potential of the amide group. These factors should be fairly constant for any amide ligand. Chelating by another functional group on the ligand and crystal packing could be other factors. To analyze if the constant factors are expressed in the geometry of cation–amide bonding, we have carried out a search in the Cambridge crystallographic database²² for the structures of amide complexes. Chelating ligands were excluded from the survey since for them the geometry of the binding depends mainly on the ligand structure. We have had also excluded observations where the O atom was bridging two cations, which was invariably found to be in the case in complexes of alkali-metal cations. Finally complexes of formamide were excluded since for this ligand the H substituent on the carbonyl carbon is much smaller than in the peptide unit.

A plot of the entry angle $M-O=C$ vs. $M-O$ distance shown in Figure 3 reveals that for smaller cations, there is a preference for cation binding at an angle $125-145^\circ$, trans to the amide nitrogen. The cations tend to be located close to the amide plane. As could be expected for transition-metal cations, where charge transfer is more significant, the direction of the $M-O$ bond is closer to the direction of the lone electron pair than for the Mg^{2+} cation. For cations with larger ionic radii, the observed angles $M-O=C$ are larger, their distribution is more scattered, and the tendency to lie in the amide plane, although still present, is less pronounced.

There is an agreement between these observations and some theoretical predictions of the mode of cation–NMA binding.²³

(22) Allen, F. H.; Bellard, S.; Brice, M. D.; Cartwright, B. A.; Doubleday, A.; Higgs, H.; Hummelink, T.; Hummelink-Peters, B. G.; Kennard, O.; Motherwell, W. D. S.; Rogers, J. R.; Watson, D. G. *Acta Crystallogr., Sect. B* 1979, *B35*, 2331–2339.

(23) Pullmann, A. *Molecular and Quantum Pharmacology*; Bergman, E., Pullman, B., Eds.; Reidel: Dordrecht, Holland, 1974; pp 401–411.

Calculation for NMA interaction with Na^+ and K^+ indeed show a minimum of ΔE for cation binding in the amide plane. In this plane there is also a very shallow minimum corresponding to the $M-O=C$ angle of about 140° , trans to the amide N atom, as observed in the structures. Those calculations do not show significant differences in the shape of this function for the Na^+ and K^+ cations; however, both of these cations have to be considered large.

The IR data are in agreement with the previous studies; the largest differences result from nitrate anions being better H-bond acceptors than Cl^- used in previous studies. As shown by frequencies of the amide band V which corresponds to N–H out-of-plane bonding,²⁴ the H bonds formed by the amide N–H group are stronger in the Mg^{2+} adduct than in the Ca^{2+} adduct. More experimental data from other structures would enable us to evaluate to what extent this is a result of stronger ligand polarization or if it reflects more efficient crystal packing.

Conclusions

The changes in the bond lengths of amides upon coordinating to alkali-earth cations are small, less than 0.01 \AA , and reflect polarization of the ligand. The degree of polarization probably affects the strength of the H bond formed by the amide N–H group. For cations with smaller ionic radii there is a preferred geometry of cation–ligand bonding at the carbonyl oxygen. It is in the amide plane, trans to the amide nitrogen, with a $M-O=C$ angle of about $135^\circ \pm 15^\circ$. For transition-metal cations this angle is smaller than for Mg^{2+} and the cation is bonded closer to the direction of the lone electron pair. For cations with larger ionic radii, in general, the orientation of the ligands is less restricted. These cations tend to bind not far from the amide plane, but the effect of lone electron pairs is less significant, and bonding occurs rather along the direction closer to the dipole moment of the amide moiety. It is possible that for macromolecular binding sites the different preferred geometry of binding of peptide oxygens by cations of different size could be a factor in specificity, or enzyme activation.

Acknowledgment. We thank Dr. E. H. Griffith for helpful discussions. This work was supported by NIH Biomedical Research Support Grants S07 RR07160 and PAN MR-19.

Registry No. $[Mg(NMA)_2(H_2O)_4](NO_3)_2$, 101998-05-4; $Ca(NO_3)_2 \cdot 4NMA$, 101998-06-5.

Supplementary Material Available: Tables of references to the structures that contain $M-O=C$ interactions discussed, tables of bond lengths, anisotropic thermal parameters, and structure factor amplitudes for $[Mg(NMA)_2(H_2O)_4](NO_3)_2$ and $Ca(NO_3)_2 \cdot 4NMA$ and table with frequencies of IR adsorption bands (31 pages). Ordering information is given on any current masthead page.

(24) Miazawa, T.; Shimanouchi, T.; Mizushima, S. *J. Chem. Phys.* 1958, *29*, 611–616.